Comprehensive Studies on Excited-State Proton Transfer of a Series of 2 - (2 ′ - Hydroxyphenyl)benzothiazole Derivatives: Synthesis, Optical Properties, and Theoretical Calculations

DATASET · SEPTEMBER 2015

5 AUTHORS, INCLUDING:

Jinling Cheng
University of Groningen
5 PUBLICATIONS **9** CITATIONS

SEE PROFILE

THE JOURNAL OF PHYSICAL CHEMISTRY C

Article

pubs.acs.org/JPCC

Comprehensive Studies on Excited-State Proton Transfer of a Series of 2-(2′-Hydroxyphenyl)benzothiazole Derivatives: Synthesis, Optical Properties, and Theoretical Calculations

Jinling Cheng,[†,‡] Di Liu,*[,†] Wei Li,[†] Lijun Bao,[†] and Keli Han[‡]

[†]State Key Laboratory of Fine Chemicals, School of Chemistry, Dalian University of Technology, 2 Linggong Road, Dalian 116024, China

[‡]State Key Laboratory of Molecular Reaction Dynamics, Dalian Institute of Chemical Physics, Chinese Academy of Sciences, 457 Zhongshan Road, Dalian 116023, People's Republic of China

Supporting Information

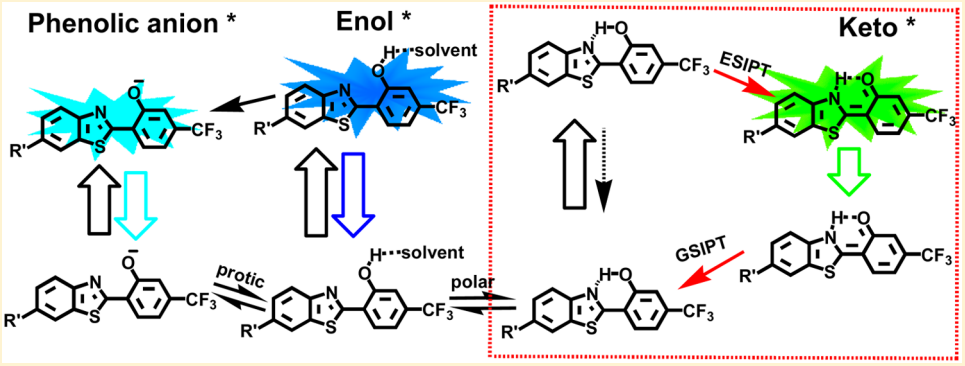

ABSTRACT: A group of novel 2-(2′-hydroxyphenyl)benzothiazole derivatives (**1**−**4**) with excited-state intramolecular proton transfer (ESIPT) character were synthesized. Their photophysical properties were studied by means of steady-state absorption and fluorescence spectra and time-resolved emission method as well as theoretical calculation in a variety of solvents. All of these compounds can yield single fluorescence at the green region in nonpolar solvents such as *n*-hexane, while dual fluorescence consisting of the blue and green bands was captured in strong polar solvents like acetonitrile. In addition, a third emission band between the former two bands was detected for these molecules simultaneously with the blue and green ones generating the well-structured triple fluorescence in protic solvent like ethanol. Systematical comparison of the fluorescence of these compounds in a series of solvents demonstrated that nonpolar solvents would facilitate ESIPT process and the green emission from the keto format, while the strong polar solvents impede the ESIPT process and favor the blue normal emission from enol. Protic solvents facilitate deprotonation and make the phenolic anion coexist with keto and enol and consequently lead to triple fluorescence. On the premise of identical keto emission intensity, the normal emission intensity of these compound increases consecutively in the order of increasing electron-withdrawing ability of the substituents regardless of solvents. The results of quantum-chemical calculations are well in line with the experimental spectra.

1. INTRODUCTION

The photoinduced proton transfer through the intramolecular hydrogen bond is defined as excited-state intramolecular proton transfer (ESIPT), which has attracted attention from both theoretical and experimental viewpoints because it has been considered to be one of the most fundamental processes involved in chemical reactions as well as in living system.[1−8] The most significant feature of the ESIPT reaction is the unique large Stokes shift emission induced by the dramatic alternation of the structure, which can reach as large as 6000−1200 cm^{-1}.[8] Because of the previously described properties, these ESIPT-possessing molecules have been applied in a variety of areas, such as functional materials (lasing materials, lighting materials),[9−12] new biotechnology (molecular recognition),[7,13,14] fluorescence imaging,[15−17] radiation scintillator,[3] and so forth.

The system greatly contributed to ESIPT research should be credited to benzothiazole type of dyes, especially the 2-(2-hydroxyphenyl)benzothiazole (HBT) group,[17,18] in which the −OH combining its conjugated group acts as the proton donor and the thiazole ring acts as the proton acceptor. The basic photophysical process of the system is demonstrated in Scheme 1.[3,11,19,20] According to our previous study, it is clear that in the nonpolar environment, based on different intramolecular

Received: November 19, 2014
Revised: February 2, 2015
Published: February 4, 2015

DOI: 10.1021/jp511578v
J. Phys. Chem. C 2015, 119, 4242−4251

Scheme 1. Characteristics of Multilevel Photocycle Scheme of the ESIPT Process

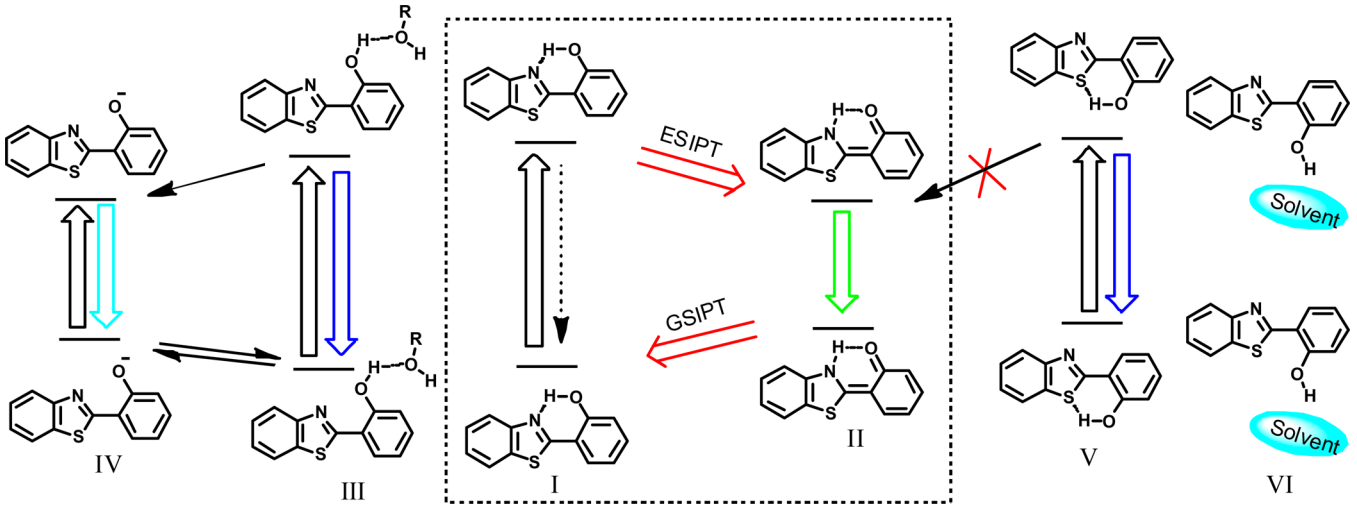

Scheme 2. Chemical Structures and Synthetic Routes for HBT Derivatives 1−4

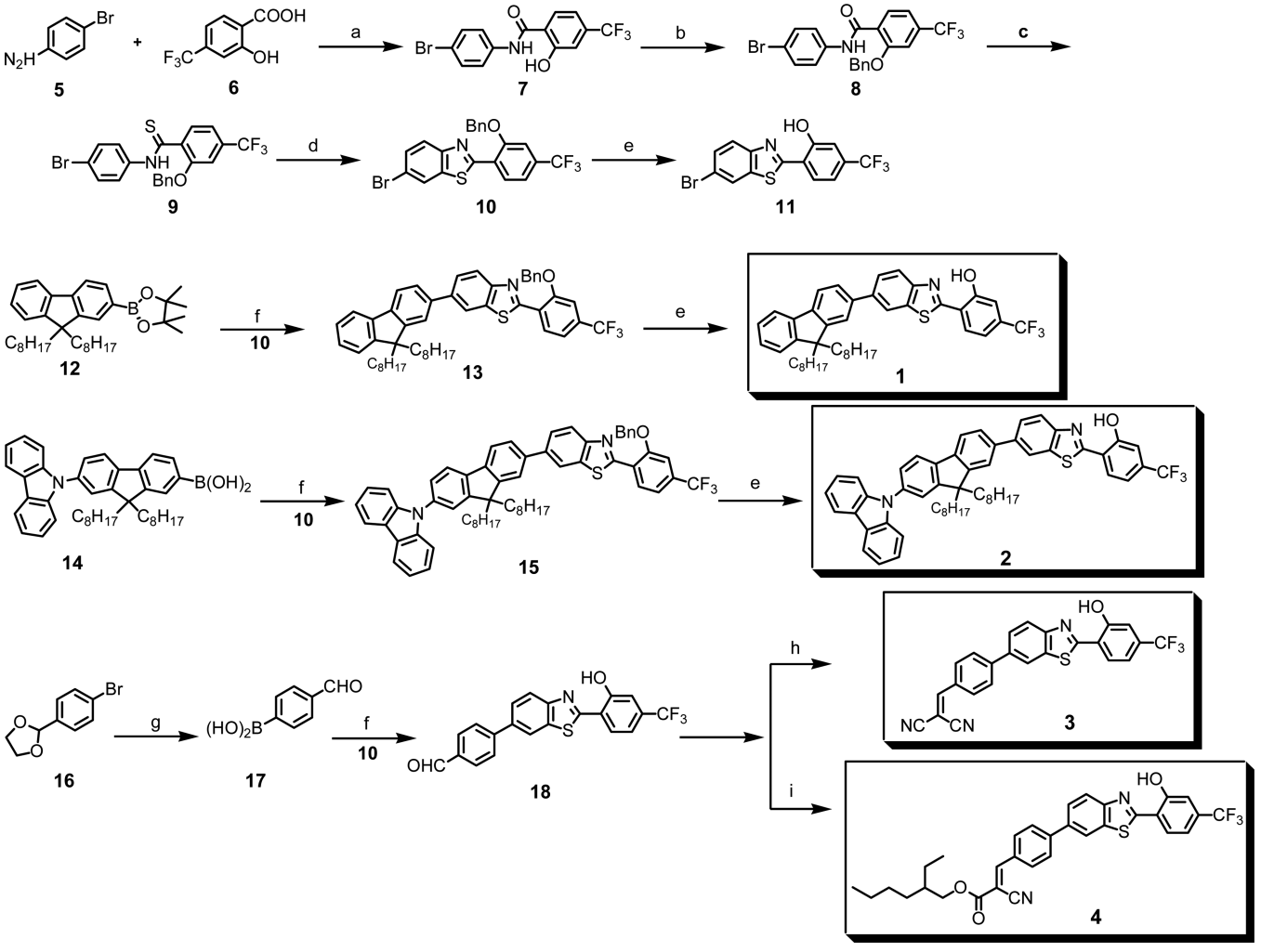

hydrogen bonds, rotamers I (cis-enol) and V (trans-enol) coexist in the ground state and rotamer I is the predominant population because it is more stable than rotamer V due to its stronger intramolecular hydrogen bond. Upon photoexcitation, however, the rotamer I undergoes an ultrafast ESIPT process (<1 ps), leading to the redistribution of electronic charge.[21] Then, a new species T* with changed electronic and nuclear configuration is generated, which finally gives out a long wavelength emission. Compared with the rotamer V, other configurations such as rotamer III and rotamer VI are more stable in more polar and protic solvents and emit a normal fluorescence in the short-wavelength region because the ESIPT

DOI: 10.1021/jp511578v
J. Phys. Chem. C 2015, 119, 4242−4251

process is terminated because of the significant distance between the proton donor and acceptor. Phenolic anions (IV) are generated as the deprotonation product of the phenolic hydroxyl group when these compounds are dissolved in protic solvents like ethanol or encountered with alkali. To the best of our knowledge, the triple fluorescence character of ESIPT molecules, which are emitted from the radiative enol and keto forms (N* and T*) and the rare deprotonated product (D*), has not yet been well-explored. This is probably because the solvation dynamics plays an important role in the ESIPT process in the ground state as well as the electronic excited states, as demonstrated by much experimental evidence including steady-state spectra and time-resolved fluorescence spectra.[12,22−25] We have reported that the ESIPT reaction and the spectral behavior of a series of HBT derivatives were quite sensitive to the solvent when it changed from nonpolar hydrocarbon to highly polar acetonitrile and even to protic ethanol.[18] In addition, although HBTs have been particularly extensively studied, most of the works focused on the characterization of the unsubstituted fluorophore platform.[26]

In the present work, we addressed these challenges through designing and synthesizing a series of novel HBT derivatives (**1**−**4**) for ESIPT studies (Scheme 2). These molecules were designed in such a way that the strong electron-withdrawing trifluoromethyl (CF_3) group was introduced into the hydroxyphenyl ring and another electron-donating or -withdrawing chromophore with large π-conjugated framework was attached to the para position of benzothiazolyl ring. The photophysical properties of these dyes were studied by means of steady-state and time-resolved fluorescence spectroscopy. The solvent effect on the spectroscopic behavior of these compounds was systematically investigated by varying the solvents from nonpolar hexane via strong polar acetonitrile to protic ethanol. The influence of the chemical structure on the photophysical properties was also studied. Quantum-chemical calculation was performed to interpret the influence of solvents and chemical structure to the photophysical properties and the ESIPT process of these HBT compounds.

2. EXPERIMENTAL METHODS

2.1. Instruments and Methods. ^{1}H NMR spectra were recorded on a 400 MHz Varian Unity Inova spectrophotometer without any peak frequencies referenced versus an internal standard (TMS) shift. Mass spectra were recorded on a Micromass Q-Tof (Micromass, Wythenshawe, U.K.) mass spectrometer equipped with an orthogonal electrospray source (Z-spray). The UV−vis absorption spectra were recorded using an HP 8453 spectrophotometer. Both the steady-state fluorescence and time-resolved fluorescence decays were measured by using a Horiba Jobin Yvon FluoroMax-4 spectrofluorometer. The time-resolved fluorescence decays were obtained using the time-correlated single photon counting (TCSPC) method, and the data analysis was performed via commercial software provided by Horiba Instruments.

2.2. Theoretical Calculations. All of the calculations were performed using the Gaussian 09 package.[27]

Geometry Optimization and UV−vis Spectra. We manually constructed geometries of compounds **1**−**4** as well as their possible tautomers. The ground state (S_0) structures of these molecules were optimized by using the density functional theory (DFT) level with B3LYP hybrid functional (which consisted of Becke's three-parameter hybrid exchange functional and the nonlocal correlation functional of Lee, Yang, and Parr (LYP)) and 6-31G** basis set,[28−30] and the vibrational frequencies at the optimized structures were calculated using the same DFT method to verify whether the optimized structures correspond to the local minima on the S_0 energy surface. Some important molecular structures of S_1 state were also obtained by using the time-dependent DFT method. To evaluate the solvent effects, *n*-hexane, acetonitrile, and ethanol were employed in the SCRF calculations by applying the polarized continuum model (PCM).[31] The Coulomb-attenuated CAM-B3LYP functional and 6-31G** basis sets were used to calculate the vertical excited energies, which can be in better agreement with the experimental results than the B3LYP hybrid function when dealing with the system with the long-range correction process.[32] We also present the calculated results for another functional named M06-2X, which will show the best overall for noncovalent interactions; however, this kind of method is very expensive and time-consuming.[33,34]

Potential Energy Curves. The ground-state potential energy surfaces along the proton transfer (GSIPT) coordinate were calculated by using the minimum energy conformer of fully optimized geometry at fixed O−H distances of hydroxyphenyl ring over the range 0.93 to 1.83 Å. The first excited state (S_1) potential energy curve (PEC) was obtained by adding the Franck−Condon transition energies from the optimized ground-state structures at fixed O−H distances to the corresponding GSIPT curve.[35]

3. RESULTS AND DISCUSSION

3.1. Design and Synthesis of Compounds. Scheme 2 illustrates the chemical structures and the synthetic routes of HBT derivatives **1**−**4**. These molecules were designed according to the following strategies. On one hand, the strong electron-withdrawing CF_3 group was introduced into the 4′-position of hydroxyphenyl ring to increase the acidity of the hydroxyl group and facilitate its deprotonation. It is expected that the introduction of this CF_3 group would alter the electronic structure and bring about innovative fluorescence behavior for these novel HBT derivatives. On the other hand, the π-conjugation framework was extended by incorporating electron-withdrawing or electron-donating aromatic groups at the 6-position of benzothiazole ring to tune the electronic state and thus the luminescence energy of the resultant molecules. For the synthesis of these compounds, the common intermediate **10** possessing the HBT skeleton and the reactive halogen site was first constructed through a multistep procedure, as shown in Scheme 2.[18,36] Condensation of 4-bromoaniline with 4-trifluoromethylsalicylic acid in the presence of PCl_3 generated the amide (**7**). After reacting with benzyl chloride to protect the phenolic hydroxyl, the amide was converted by Lawesson's reagent into the thiobenzamide (**9**). Jacboson reaction of this thiobenzamide with potassium ferricyanide resulted in the important intermediate 2-(2′-(benzyloxy)-4′-(trifluoromethyl)phenyl)-6-bromobenzothiazole (**10**). Finally, the Suzuki coupling reaction of **10** with the borinic acid **12** or **14** followed by deprotection of hydroxyl group generated the corresponding target compound **1** or **2**.[37−41] After Suzuki coupling reaction, **3** and **4** were obtained through the Knoevenagel condensation reaction between the aldehyde group on intermediate **18** with malononitrile or octan-3-yl 2-cyanoacetate. The detailed synthetic procedure and characterization of these compounds are provided in the Supporting Information (SI). All of these compounds have good solubility in common organic solvents so that they could

DOI: 10.1021/jp511578v
J. Phys. Chem. C 2015, 119, 4242−4251

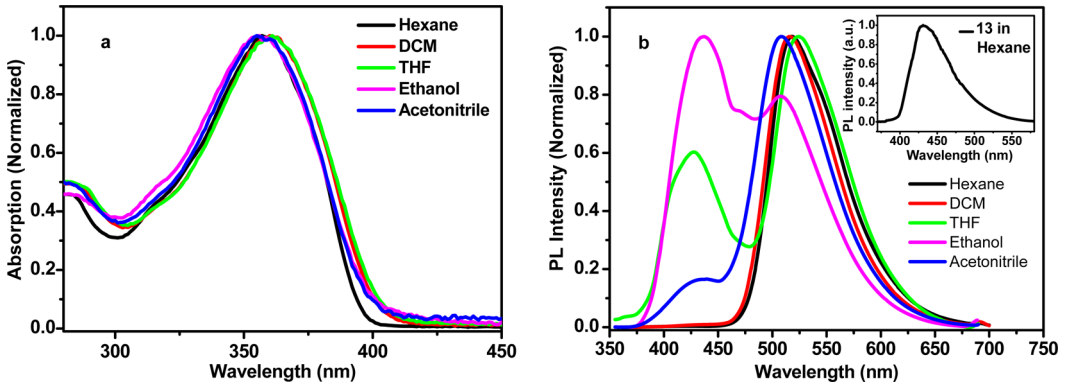

Figure 1. Steady-state absorption (a) and fluorescence (b) spectra of compound **1** in different solvents at room temperature. Inset in panel b is the fluorescence spectrum of the reference compound **13** in hexane.

Scheme 3. Optimized Structures for Compounds 1−4 on S_0 State[a]

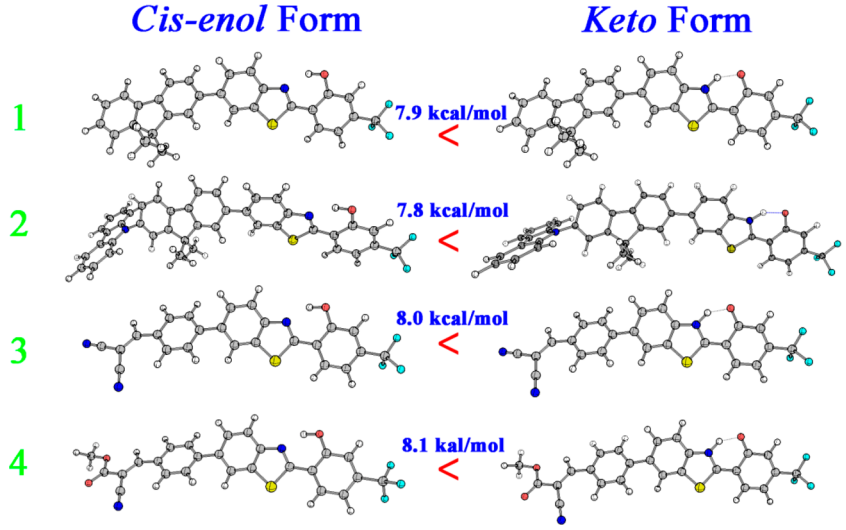

[a]Colors: white, H; red, O; blue, N; yellow, S; cyan, F; gray, C. (For compounds **1** and **2** the $-C_8H_{17}$ are represented by $-CH_3$ to simplify the calculation.)

be well-purified for spectral study. Before spectral study, the thermal stability of these compounds was investigated by means of thermogravimetric analysis (TGA). As shown by the Figure S1 in the SI, all of these four compounds have good thermal stability with decomposition temperatures (corresponding to 5% weight loss) of 321, 359, 254, and 317 °C, respectively. It is interesting that the thermal stability of these compounds shows approximately linear proportion to their molecular weight.

3.2. Steady-State Approach. The steady-state absorption and fluorescence spectra of compounds **1**−**4** in various solvents at room temperature are shown in Figure 1 and Figures S2−S4 in the SI. The absorption spectra of all of these compounds in various solvents are characterized by a broad band with peaks at 360−370 nm, which can be ascribed to the $\pi-\pi^*$ transition of the conjugated backbone of these molecules. With increasing solvent polarity from *n*-hexane to acetonitrile, the spectral profile and position of these absorption spectra almost remain unchanged, implying little influence of solvent polarity to the ground states of these compounds. The single absorption band indicates that these derivatives are mainly maintained at their enol-forms at the ground state and insensitive to the surrounding media. Supplementary support of the previously described experimental results is provided by the computational approaches. The ground-state potential energies calculated at B3LYP/6-31G (d, p) level are shown in Scheme 3. It is observed that the normal forms (i.e., cis-enol) of all of these compounds are the dominant ground-state species due to their lower energy than their tautomer forms (keto) by 7.8 to 8.1 kcal/mol. The calculated excitation energy and absorption wavelength of each compound summarized in Table S1 in the SI are close to the above experimental values, further confirming that enol forms are the predominant species of these HBT derivatives in various solvents at the ground state.

Upon photoexcitation at the absorption maxima, these HBT derivatives exhibit different fluorescence properties with varying the solvent polarity. For example, in nonpolar hexane, compound **1** emits single fluorescence with the emission peak at 517 nm (Figure 1b) and a large Stokes shift of ca.160 nm. With increasing solvent polarity, for example, in tetrahydrofuran and acetonitrile, a short-wavelength band at 430 nm was detected along with the original band at ∼517 nm, leading to the formation of the dual fluorescence (Figure 1b). To verify the origin of these two emission bands, the reference compound **13** that has the identical molecular skeleton to molecule **1** but with protected phenolic hydroxy was studied under identical conditions for comparison. As shown in the

DOI: 10.1021/jp511578v
J. Phys. Chem. C 2015, 119, 4242−4251

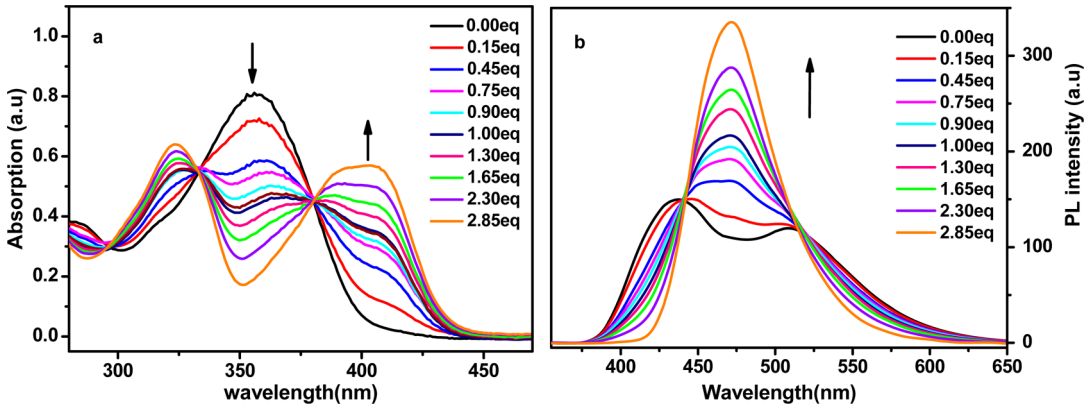

Figure 2. Changes in the UV−vis absorption (a) and emission spectra (b) for compound **1** (3.00×10^{-5} mol/L) in ethanol with the addition of $[(Bu)_4N]^+OH^-$ (1.86×10^{-3} mol/L).

Table 1. Summary of Excited-State Lifetimes at Two Different Probing Wavelengths for Compounds 1−4 in Various Solvents (Ethanol, Acetonitrile, and *n*-Hexane)

		ethanol			acetonitrile			*n*-hexane		
	probing wavelength (nm)	τ_1/ps	τ_2/ns	CHISQ	τ_1/ps	τ_2/ns	CHISQ	τ_1/ps	τ_2/ns	CHISQ
1	430	109 (0.20)	1.33 (0.80)	1.12	105 (0.41)	1.55 (0.59)	1.10	100 (0.49)	2.93 (0.51)	1.20
	515	624 (0.34)	2.68 (0.66)	1.35	178 (0.56)	1.03 (0.44)	1.32	59.3 (0.16)	2.84 (0.84)	1.35
2	430	115 (0.18)	1.99 (0.82)	1.28	105 (0.48)	1.55 (0.52)	1.10	872 (0.02)	1.97 (0.98)	1.20
	515	388 (0.24)	2.19 (0.76)	1.35	434 (0.71)	1.40 (0.39)	1.32		2.46 (1.00)	1.35
3	430	35 (0.90)	3.33 (0.10)		[a]	[a]	[a]	143 (0.40)	1.94 (0.60)	1.10
	525	397 (0.96)	2.45 (0.04)	1.27	197 (0.95)	0.94 (0.05)	1.37		1.72 (1.00)	1.49
4	430	35 (0.84)	2.07 (0.16)	1.72	146 (0.88)	4.63 (0.12)	1.31	177 (0.40)	2.17 (0.60)	1.10
	515	159 (0.94)	2.63 (0.06)	1.27	32 (0.98)	4.77 (0.02)	1.37	136 (0.12)	1.96 (0.88)	1.35

[a]Not determined due to the instrumental resolution.

inset of Figure 1b, the single fluorescence of compound **13** is peaked at 432 nm, which should correspond to the $S_1 \rightarrow S_0$ transition of the conjugated backbone of this molecule. The different fluorescence spectra of compounds **1** and **13** confirm the important role of the phenolic hydroxy group to the emissive behavior of **1**. According to the typical spectral features of the general HBT derivatives,[8] it is safe to ascribe the above 430 and 517 nm emission bands of compound **1** in different solvents to the corresponding excited states of enol form III and keto form II,[42] respectively. In nonpolar or weak polar solvents, the strong intramolecular hydrogen bonding stabilizes the cis-enol rotamer I and makes it the major population at the ground state. Upon photoexcitation, this enol undergoes ESIPT to form the excited state of lower energy keto tautomer II that then emits fluorescence at longer wavelength (517 nm). It is obvious that the tautomerization from enol to keto through ESIPT process results in the large Stokes shift of these HBT molecules. With increasing solvent polarity, such as in tetrahydrofuran or acetonitrile, the intermolecular hydrogen bonding between molecule **1** and the solvent competes with the intramolecular hydrogen bonding, enhancing the population of conformer III and consequently increasing its normal fluorescence intensity at short wavelength (430 nm). Furthermore, when **1** is dropped into protic ethanol, a third emission band at 470 nm can be simultaneously detected, accompanied by the original green (517 nm) and further enhanced blue (430 nm) bands (Figure 1b). The triple fluorescence covering a wide spectral range from 400 to 600 nm is generated. The similar spectral evolution from single via dual finally to triple fluorescence was observed for the other three compounds **2**, **3**, and **4** when varying the solvent polarity consecutively, as shown by the fluorescence spectra in Figures S2−S4 in the SI.

For the triple fluorescence in protic solvent, according to our DFT previous calculation,[21] the third emission band at ∼470 nm could be ascribed to the corresponding phenolic anion IV ($[PhO^-]$) that is generated due to deprotonation induced by the intermolecular hydrogen bonding between the phenolic hydroxy and the solvent molecules. To give solid evidence of the generation of phenolic anion, we monitored the fluorescence spectra of these compounds when titrated with $[(Bu)_4N]^+OH^-$ (from 0.00 to 2.85 equiv) in ethanol as well as in other solvents (tetrahydrofuran and acetonitrile, Figure S6 in the SI). Figure 2 illustrates the changes of both the absorption

DOI: 10.1021/jp511578v
J. Phys. Chem. C 2015, 119, 4242−4251

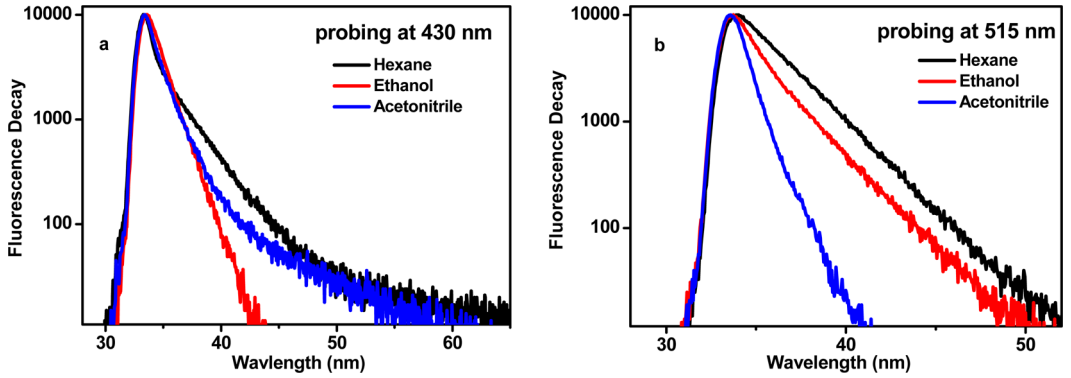

Figure 3. Time-resolved fluorescence decays of compound **1** in *n*-hexane, ethanol, and acetonitrile monitored at (a) 430 and (b) 515 nm.

and fluorescence spectra of compound **1** as an example when titrated with $[(Bu)_4N]^+OH^-$ in ethanol. With the addition of $[(Bu)_4N]^+OH^-$, the main absorption band at ~356 nm collapsed and was replaced by two new bands at 324 and 408 nm; at the same time, the fluorescence spectral profile changed from the triple fluorescence (at 430, 470, and 512 nm) gradually into the single fluorescence with the central band at 470 nm predominating the spectra. The simultaneous appearance of the isoelectric point in both absorption and fluorescence spectra indicates the generation of new chemical species with the addition of the alkali. On the basis of the common sense of chemical reactions, it would be reasonable to assign the new absorption bands at 324 and 408 nm and the fluorescence band at 470 nm to the phenolic anion of compound **1**. It is understandable that both the tautomer emission at long wavelength and the normal emission at short wavelength decreased with the increasing alkali fraction in ethanol because the high concentration of alkali must consume almost all of the molecules in the enol format, including I, V, and III, and convert them into the luminescent anion IV. All other derivatives, **2**−**4**, were studied in a similar way, and similar results were observed, as shown by the spectra changes upon titration with $[(Bu)_4N]^+OH^-$) in Figures S5−S7 in the SI.

3.3. Time-Resolved Fluorescence Spectra. The time-resolved fluorescence of these compounds was monitored at both enol and keto emission bands in different solvents to investigate detailed ESIPT dynamic. For brevity, we restrict the comparison here in three solvents in terms of nonpolar *n*-hexane, strong polar acetonitrile, and protic ethanol. The time-resolved decays monitored at both the enol and the keto emissions were characterized by biexponential, a short-lived component (τ_1) and the other contribution from the long-lived component (τ_2) (some exceptions also exist) (Table 1). Take compound **1**, for instance: When monitored at 430 nm in the protic solvents, the main component of the fluorescence decay consists of a slow decay time of 1.33 ns (47.9%) and a faster decay time of 109 ps (52.1%). On the fast time scales, a slight growth is observed as the polarity of solvent increased from hexane to acetonitrile and then to ethanol, which demonstrates that the polarity of the solvent or the hydrogen bond of the protic solvents impedes the ESIPT process. In the case of the excitation spectrum recorded at the maximum of the lower energy emission band, the decay times of 624 ps (33.76%) and 2.68 ns (66.24%) were observed in ethanol, and the longest lifetime was detected in *n*-hexane, implying the smallest effect of the solvation. However, the lifetime on the picosecond time scale is confined by the instrumental resolution of 200 ps.

Figure 3 illustrates the time-resolved decay profiles of **1** monitored at different wavelengths in the previously described three solvents. Our investigation is mainly focused on the descending of the fluorescence intensity. First of all, the spectrum of the decay when monitored at short wavelength should be assigned to the collaborative effects of the fluorescence decay of the enol* form and the ESIPT process. The intensity of enol* emission is greatly reduced in *n*-hexane, implying a faster ESIPT process than that in the other two kinds of solvents on the ultrafast time scales, while in ethanol, a strong hydrogen-bond-donating solvent is used, as the slowest proton-transfer dynamics is observed. When monitored at the keto* emission (515 nm for compounds **1**, **2**, and **4**; 525 nm for compound **3**), time-resolved decay characterized by the inactivation of keto*, predominately, reveals an entirely different quench process in these three different solvents. In nonpolar solvent *n*-hexane, the slowest time course of the decays (the long-lived ones) suggests that the interaction between the solvent molecular and solute molecular is insignificant. Then, in the protic ethanol, the rate of the inactivation enhances; moreover, the quickest descent of the curve is observed in strong polar solvent acetonitrile, verifying that the interaction between the solvent and solute stimulate the quench of the keto*. The time-resolved fluorescence spectra of other compounds were quite similar in terms of time constant and profile to compound **1** in these solvents (Table 1 and Figures S8−S10 in the SI).

3.4. Theoretical Calculations for ESIPT Mechanism. To understand the relationship between molecular structures and the ESIPT process and the spectroscopic properties of these compounds, we carried out theoretical calculation for the cis-enol form (I in Scheme 1) of these compounds with DFT method. In the ground state, the O−H bond lengths of phenolic hydroxy group are calculated at the B3LYP/6-31G(d,p) level as 0.9966, 0.9965, 0.9960, and 0.9958 Å for **1**−**4**, respectively. At the same time, the intramolecular hydrogen bond N···H lengths are calculated as 1.7099, 1.7106, 1.7154, and 1.7126 Å. After excitation to the S1 state, the O−H bond lengths are extended to 1.0128, 0.9995, and 0.9997 Å for compounds **1**, **2**, and **4**, while that for compound **3** decreased to 0.9934 Å. Those for N···H bonds decreased to 1.6885, 1.6924, 1.7086, and 1.7032 Å for **1**−**4**. The consecutive increase in O−H bond length (except compound **3**) and the consecutive decrease in N···H bond length suggest the increase in intramolecular hydrogen bond strength after excitation to the

DOI: 10.1021/jp511578v
J. Phys. Chem. C 2015, 119, 4242−4251

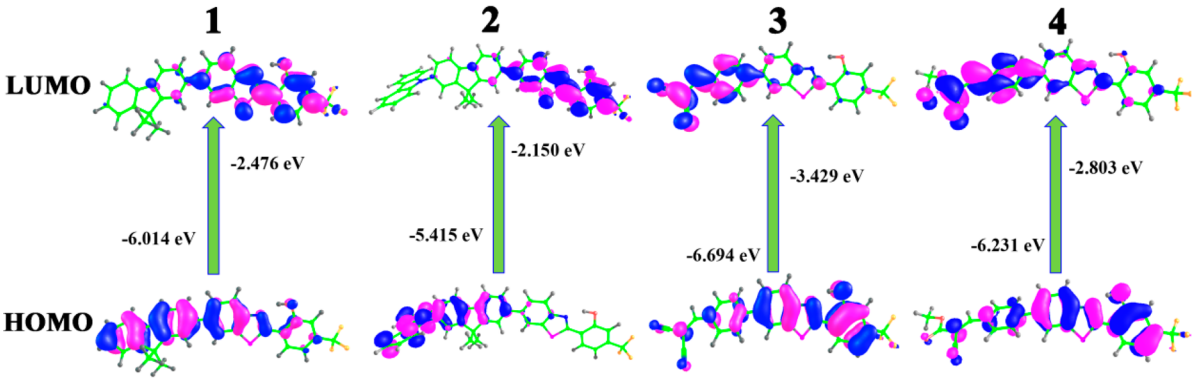

Figure 4. Frontier molecular orbitals involved in crucial electronic excitations and corresponding energy levels of compounds **1**−**4** calculated by B3LYP.

S_1 state, which will definitely favor the ESIPT process. It should be noted that the dihedral angles (φ) between the substituent group and the HBT unit for compounds **1** and **2** are 37.47 and 34.29°, while the φ values for compounds **3** and **4** are much smaller, 17.82 and 16.33°, respectively, implying that compounds **3** and **4** have more efficient conjugation between the substituent groups and HBT unit than analogues **1** and **2**. This is consistent with the previous bond length analysis because the highly electron-withdrawing substituent groups (CN) in molecules **3** and **4** can take effect through more efficient conjugation to reduce the electron density on N atoms and finally lead to longer N···H hydrogen bonds and shorter O−H bonds at both ground and excited states. Table S2 in the SI compares performance on calculating the length for hydrogen bonds by B3LYP and M06-2X; both of them present similar results and agree well with our experimental results. Later we continued to adapt the B3LYP functional for other simulations because it is less time-consuming.

For more microcosmic details, we should refer to the orbital analysis. As illustrated in Figure 4, for compounds **1** and **2**, their highest occupied molecular orbitals (HOMOs) are mainly located on the benzothiazole ring and the substituent groups, with more contribution from the triphenylamino group for **2**, while their lowest unoccupied molecular orbitals (LUMOs) mainly distributed on the trifluoromethylbenzyl ring. This is reasonable because the trifluoromethylbenzyl ring together with the benzothiazole rings stands for the electron-deficient part, and the fluorene or triphenylamino-substituted fluorene is an electron-rich moiety in these molecules. However, with the introduction of the strong electron-withdrawing cyano groups in molecules **3** and **4**, their HOMO spread over the whole molecular skeleton, and their LUMO shifted to the cyano-containing terminal of both molecules.

On the basis of the preivous results triggered by ESIPT, an overall proton-transfer cycle of these derivatives can thus be depicted in Figure 5 and Figures S11−S13 in the SI. Take **1**, for example: In the intrinsic six-membered-ring cycle induced by intramolecular hydrogen bond, the enol-form represents the most stable structure, while the keto-form has the highest instability with high-energy barrier (7.90 kcal/mol in acetonitrile and 9.6 kcal/mol in *n*-hexane), which suggests the nonviability of the GSIPT process. Upon photoexcitation via light energy absorption, the phenolic proton in molecule **1** undergoes an ultrafast transfer to the acceptor N atom after overcoming a small energy barrier of 0.9 kcal/mol in hexane, generating the excited state of the lower energy keto-tautomer.

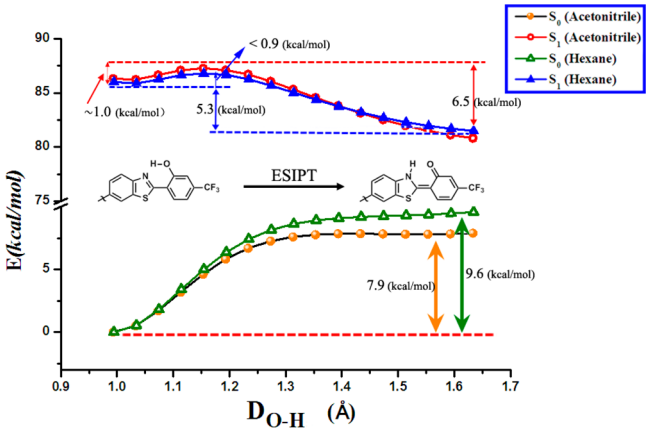

Figure 5. Potential energy curves from enol-form to keto-form of the compound **1** at the excited state and ground state in two different solvents (*n*-hexane and acetonitrile).

Interestingly, in a more polar solvent such as acetonitrile, as indicated in Figure 5, the energy gap for proton transfer has been slightly increased to >1 kcal/mol, which should be attributed to the solvent effects (such as the dipole moment change). As shown in Figures S11−S13 in the SI, the ESIPT process is barrierless for compound **2**, while for **3** and **4**, the energy gaps climb to 3.4 and 3.0 kcal/mol, respectively, implying less efficient proton transfer.

3.5. Substituent and Solvent Effects on ESIPT Process and Photophysics. On the basis of the previous discussion, ESIPT dynamics and the spectroscopic behavior may be due to a combination of two effects: substituent and solvent effects. Figure 6 illustrates the fluorescence spectra of these four compounds in dichloromethane. It is obvious that compound **1** emits single fluorescence from keto and the other three analogues emit dual fluorescence from both keto and enol. When normalized at the keto emission peak, the enol-form emission intensity increases in the order of **1**, **2**, **4**, and **3**, which is just in the order of increasing electron-withdrawing ability of the substituents at the six-site of benzothiazole ring.

The specific substituent effects on ESIPT dynamics can be well explained by the theoretical calculation results. In the case of compounds **1** and **2**, HOMO is mainly located on the benzothiazole and the electron donating triphenylamine unit, while the LUMO orbital tend to the distribute on the benzothiazole and CF_3 groups because of the strong electron withdrawing property of CF_3 group. After being excited to S_1

DOI: 10.1021/jp511578v
J. Phys. Chem. C 2015, 119, 4242−4251

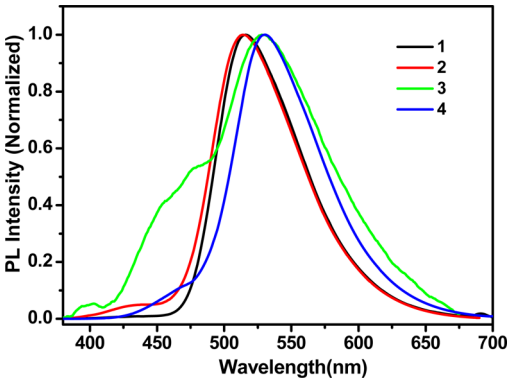

Figure 6. Normalized fluorescence spectra for compounds **1**−**4** in dichloromethane at room temperature (λ_{ex} = 345 nm).

state, the most noticeable character is the extent of the electron density surrounding atom N of benzothiazole groups (Figure 4), enhancing the attraction between N and H atoms and the intramolecular hydrogen bonds, thus the energy barrier for proton transfer is very low as shown in the PECs (Figure 6 and Figure S11 in the SI). Consequently the ESIPT is efficient and the long-wavelength keto emission is relatively strong. For compound **2**, the energy barrier for proton transfer (almost zero, Figure S11 in the SI) is smaller than that of compound **1**. This is because the incorporation of strong electron-donating triphenylamino group must increase the charge density on N atom and thus more favor the ESIPT process. However, the ratio of long-wavelength keto emission to enol emission for molecule **2** is unexpectedly lower than that of **1**. The true reason for this point is still unknown currently and should depend on a more experimental and theoretical study. In the case of compounds **3** and **4**, the electron density in the HOMO is located on the whole molecule, while the LUMO is distributed mainly on the substituent terminal due to the introduction of highly electron-withdrawing CN groups (Figure 4). The most noticeable difference is the small extent of the LUMO surrounding N atom, which results in the sharp decrease in the attraction between H and N atoms and greatly increased energy barriers required for proton transfer (3.4 and 3.0 kcal/mol for compounds **3** and **4**, respectively, Figures S12 and S13 in the SI). The substituent effect in compounds **3** and **4** can be further verified by their extended N···H bond lengths at both ground state and excited state in comparison with **1** and **2**. Compounds **3** and **4** exhibit normal emission with certain intensity even in nonpolar hexane (Figures S3 and S4 in the SI), while **1** and **2** only emit keto emission (Figure 1 and Figure S2 in the SI) in same solvent. This is also because of the stronger electron-withdrawing effect of the substituents in molecules **3** and **4**. In addition, it should be noted that the keto emission of compounds **3** and **4** is a little red-shifted relative to that of **1** and **2**. This should be because although the electron-withdrawing and -donating groups exist on each side of HBT unit in molecules **1** and **2**, they do not form an effective conjugation due to twisted molecular configuration with the dihedral angles >30°. However, for compounds **3** and **4**, effective conjugation is achieved due to more planar molecular configuration with smaller dihedral angles, resulting in intramolecualr charge transfer between the strong electron-withdrawing CN side and the HBT side and consequently leading to bathochromic effect in fluorescence. These experimental and theoretical studies combine to verify the substituent effect that the electron-donating substituents at the six-site of the HBT ring favor the ESIPT process and keto tautomer emission, while the electron-withdrawing groups at the same position suppress the ESIPT reaction.

Comparison of the absorption and fluorescence spectra of each compound in different solvents reveals the influence of the solvent to the ESIPT process and the spectroscopic behavior. Compound **1** is selected as the example again for discussion. As shown in Figure 1a, the profile and position of the absorption spectra are almost independent of the solvent polarity, indicating the little influence of the solvent on the ground state of this HBT molecule. However, the fluorescence spectra are quite sensitive to the solvent polarity, as shown in Figure 1b. The emission of **1** evolves from single fluorescence in nonpolar or weak polar solvents via dual fluorescence in strong polar acetonitrile to triple fluorescence in ethanol. The further decrease in solvent polarity results in a further increase in the tautomer emission. According to our time-resolved fluorescence results, the nonpolar solvent plays a little influence on the ESIPT process because solute−solvent interaction could be insignificant. However, in the case of strong polar solvent such as acetonitrile, it is clear that the polar solvent favors the normal emission despite the electron-withdrawing or -donating nature of the substituent groups in molecules **1**−**4**. The difference is attributed to two elements: one is the solvent polarity effect on the photophysical properties and the other is the H-bond interactions between solute and solvent molecules. In addition, because of the introduction of the $-CF_3$ group, a distinct decrease in the electron density on the O atom can be observed, which will definitely increase the acidity of the hydroxy group and facilitate its deprotonation in protic ethanol. Our experimental and calculated results demonstrated that polar solvents favor the normal emission, while nonpolar solvents facilitate ESIPT process and tautomer emission. Above all, in our present work, the systematical comparison of both the substituent effect and the solvent effect indicates that the solvent is the more effective factor to determine the ESIPT reaction and fluorescence properties, although substituents have important influences on the ESIPT process and fluorescence behaviors as well.

4. CONCLUSIONS

In summary, a series of novel ESIPT molecules **1**−**4** based on the HBT unit were synthesized for the first time, which have an electron-donating or -withdrawing substituent on the six-site of the benzothiazole ring. The spectroscopic experiments and quantum-chemistry calculations have been employed to investigate the photophysical properties of these compounds. The introduction of CF_3 in the hydroxyphenyl ring evidently promotes the acidity of the hydroxyl group and consequently facilitates its deprotonation and finally results in the generation of precious triple fluorescence from the enol, keto, and phenolic anions. The most important advantage of the present triple fluorescence over other triple fluorescence system in literature reports lies in the easy achievement of the triple fluorescence from a single ESIPT molecule under so mild conditions. The substituent effect and solvent effect on the ESIPT dynamics and the spectroscopic properties are investigated theoretically and experimentally. It is observed that strong electron-withdrawing groups at the six-site of benzothiazole ring would suppress the ESIPT process and favor the enol emission, while the electron-donating groups at the same position would facilitate ESIPT process and favor the keto tautomer emission. It is always true

DOI: 10.1021/jp511578v
J. Phys. Chem. C 2015, 119, 4242−4251

that the polar solvents suppress the ESIPT process and favor the normal emission despite the electron-withdrawing or -donating nature of the substituent groups. Each HBT derivative in the present study encountered a common spectral evolution from single fluorescence to dual fluorescence and further to triple fluorescence with solvent going from nonpolar to polar and to protic. It also can be concluded that the solvent effect, rather than substituent factor, plays an essential role in determining the ESIPT process and the fluorescence behaviors.

■ ASSOCIATED CONTENT

Supporting Information

Compound syntheses, TGA curves for compounds **1**−**4**, steady-state absorption and fluorescence spectra of compounds **2**−**4**, changes in the UV−vis and emission spectra for compounds **2**−**4**, time-resolved fluorescence decays of compounds **2**−**4**, potential energy curves from enol-form to keto-form of the compounds **2**−**4**, calculated photophysical parameters of compounds **1**−**4**, and comparison of calculated O−H and N−H bonds of compounds **1**−**4**. This material is available free of charge via the Internet at http://pubs.acs.org.

■ AUTHOR INFORMATION

Corresponding Author

*E-mail: liudi@dlut.edu.cn.

Notes

The authors declare no competing financial interest.

■ ACKNOWLEDGMENTS

We thank the National Natural Science Foundation of China (21274016, 21374013, and 21421005), the Program for Changjiang Scholars and Innovative Research Team in University (IRT-13R06) and Program for DUT Innovative Research Team (DUT2013TB07), and the Fundamental Research Funds for the Central Universities (DUT13LK06 and DUT12ZD211) for financial support of this work.

■ REFERENCES

(1) Choi, K.; Hamilton, A. D. A Dual Channel Fluorescence Chemosensor for Anions Involving Intermolecular Excited State Proton Transfer. *Angew. Chem., Int. Ed.* **2001**, *40*, 3912−3915.

(2) Hammes-Schiffer, S.; Stuchebrukhov, A. A. Theory of Coupled Electron and Proton Transfer Reactions. *Chem. Rev.* **2010**, *110*, 6939−6960.

(3) Kwon, J. E.; Park, S. Y. Advanced Organic Optoelectronic Materials: Harnessing Excited-State Intramolecular Proton Transfer (ESIPT) Process. *Adv. Mater.* **2011**, *23*, 3615−3642.

(4) Lukeman, M.; Wan, P. Excited-State Intramolecular Proton Transfer in o-hydroxybiaryls: A New Route to Dihydroaromatic Compounds. *J. Am. Chem. Soc.* **2003**, *125*, 1164−1165.

(5) Meyer, T. J.; Huynh, M. H. V.; Thorp, H. H. The Possible Role of Proton-Coupled Electron Transfer (PCET) in Water Oxidation by Photosystem II. *Angew. Chem., Int. Ed.* **2007**, *46*, 5284−5304.

(6) Park, S.; Seo, J.; Kim, S. H.; Park, S. Y. Tetraphenylimidazole-Based Excited-State Intramolecular Proton-Transfer Molecules for Highly Efficient Blue Electroluminescence. *Adv. Funct. Mater.* **2008**, *18*, 726−731.

(7) Zhao, G.; Han, K. Hydrogen Bonding in the Electronic Excited State. *Acc. Chem. Res.* **2011**, *45*, 404−413.

(8) Zhao, J.; Ji, S.; Chen, Y.; Guo, H.; Yang, P. Excited State Intramolecular Proton Transfer (ESIPT): from Principal Photophysics to the Development of New Chromophores and Applications in Fluorescent Molecular Probes and Luminescent Materials. *Phys. Chem. Chem. Phys.* **2012**, *14*, 8803−8817.

(9) D'Andrade, B. W.; Holmes, R. J.; Forrest, S. R. Efficient Organic Electrophosphorescent White-Light-Emitting Device with a Triple Doped Emissive Laye. *Adv. Mater.* **2004**, *16*, 624−731.

(10) Kim, T. H.; Lee, H. K.; Park, O. O.; Chin, B. D.; Lee, S. H.; Kim, J. K. White-Light-Emittig Diodes Based on Iridium Complexes via Efficient Energy Transfer from a Conjugated Polymer. *Adv. Funct. Mater.* **2006**, *16*, 611−617.

(11) Park, S.; Kwon, J. E.; Kim, S. H.; Seo, J.; Chung, K.; Park, S.-Y.; Jang, D.-J.; Medina, B. a. M. n.; Gierschner, J.; Park, S. Y. A White-Light-Emitting Molecule: Frustrated Energy Transfer between Constituent Emitting Centers. *J. Am. Chem. Soc.* **2009**, *131*, 14043−14049.

(12) Sun, W.; Li, S.; Hu, R.; Qian, Y.; Wang, S.; Yang, G. Understanding Solvent Effects on Luminescent Properties of a Triple Fluorescent ESIPT Compound and Application for White Light Emission. *J. Phys. Chem. A* **2009**, *113*, 5888−5895.

(13) Kim, S. K.; Lee, D. H.; Hong, J.-I.; Yoon, J. Chemosensors for Pyrophosphate. *Acc. Chem. Res.* **2008**, *42*, 23−31.

(14) Wu, J.; Liu, W.; Ge, J.; Zhang, H.; Wang, P. New Sensing Mechanisms for Design of Fluorescent Chemosensors Emerging in Recent Years. *Chem. Soc. Rev.* **2011**, *40*, 3483−3495.

(15) Kim, S.; Park, S. Y. Photochemically Gated Protonation Effected by Intramolecular Hydrogen Bonding: Towards Stable Fluorescence Imaging in Polymer Films. *Adv. Mater.* **2003**, *15*, 1341−1344.

(16) Lim, S.-J.; Seo, J.; Park, S. Y. Photochromic Switching of Excited-State Intramolecular Proton-Transfer (ESIPT) Fluorescence: A Unique Route to High-Contrast Memory Switching and Non-destructive Readout. *J. Am. Chem. Soc.* **2006**, *128*, 14542−14547.

(17) Park, S.; Kim, S.; Seo, J.; Park, S. Y. Strongly Fluorescent and Thermally Stable Functional Polybenzoxazole Film: Excited-state Intramolecular Proton Transfer and Chemically Amplified Photo-patterning. *Macromolecules* **2005**, *38*, 4557−4559.

(18) Wang, R.; Liu, D.; Xu, K.; Li, J. Substituent and Solvent Effects on Excited State Intramolecular Proton Transfer in Novel 2-(2′-Hydroxyphenyl)benzothiazole Derivatives. *J. Photochem. Photobiol., A* **2009**, *205*, 61−69.

(19) Abou-Zied, O. K.; Jimenez, R.; Thompson, E. H.; Millar, D. P.; Romesberg, F. E. Solvent-Dependent Photoinduced Tautomerization of 2-(2 ′-Hydroxyphenyl)benzoxazole. *J. Phys. Chem. A* **2002**, *106*, 3665−3672.

(20) Rodríguez, M. C. R.; Penedo, J. C.; Willemse, R. J.; Mosquera, M.; Rodríguez-Prieto, F. On the Mechanism of Alcohol-Catalyzed Excited-State Intramolecular Proton Transfer in Cationic Benzimidazoles. *J. Phys. Chem. A* **1999**, *103*, 7236−7243.

(21) Cheng, J.; Liu, D.; Bao, L.; Xu, K.; Yang, Y.; Han, K. A Single 2-(2′-Hydroxyphenyl)benzothiazole Derivative Can Achieve Pure White-Light Emission. *Chem. Asian. J.* **2014**, *9*, 3215−3220.

(22) Collins, G. E.; Choi, L. S.; Callahan, J. H. Effect of Solvent Polarity, pH, and Metal Complexation on the Triple Fluorescence of 4-(N-1,4,8,11-Tetraazacyclotetradecyl)benzonitrile. *J. Am. Chem. Soc.* **1998**, *120*, 1474−1478.

(23) Hazra, A.; Soudackov, A. V.; Hammes-Schiffer, S. Isotope Effects on the Nonequilibrium Dynamics of Ultrafast Photoinduced Proton-Coupled Electron Transfer Reactions in Solution. *J. Phys. Chem. Lett.* **2010**, *2*, 36−40.

(24) Kruk, M.; Ngo, T. H.; Savva, V.; Starukhin, A.; Dehaen, W.; Maes, W. Solvent-Dependent Deprotonation of meso-Pyrimidinylcorroles: Absorption and Fluorescence Studies. *J. Phys. Chem. A* **2012**, *116*, 10704−10711.

(25) Singh, R. B.; Mahanta, S.; Guchhait, N. Solvent Dependent Excited State Spectral Properties of 4-Hydroxyacridine: Evidence for Only Water Mediated Excited State Proton Transfer Process. *J. Photochem. Photobiol., A* **2008**, *200*, 325−333.

(26) Lochbrunner, S.; Wurzer, A. J.; Riedle, E. Microscopic Mechanism of Ultrafast Excited-State Intramolecular Proton Transfer: A 30-fs Study of 2-(2′-Hydroxyphenyl)benzothiazole. *J. Phys.Chem. A* **2003**, *107*, 10580−10590.

(27) Frisch, M.; Trucks, G. W.; Schlegel, H. B.; Scuseria, G. E.; Robb, M. A.; Cheeseman, J. R.; Scalmani, G.; Barone, V.; Mennucci, B.;

DOI: 10.1021/jp511578v
J. Phys. Chem. C 2015, 119, 4242−4251

Petersson, G. A. *Gaussian 09*, revision A.02; Gaussian, Inc.: Wallingford, CT, 2009; p 34.
(28) Becke, A. D. Density-Functional Exchange-Energy Approximation with Correct Asymptotic Behavior. *Phys. Rev. A* **1988**, *38*, 3098−3100.
(29) Becke, A. D. Density-Functional Thermochemistry. III. The Role of Exact Exchange. *J. Chem. Phys.* **1993**, *98*, 5648−5652.
(30) Lee, C.; Yang, W.; Parr, R. G. Development of the Colle-Salvetti Correlation-Energy Formula into a Functional of the Flectron Density. *Phys. Rev. B* **1988**, *37*, 785−789.
(31) Cossi, M.; Barone, V.; Mennucci, B.; Tomasi, J. Ab Initio Study of Ionic Solutions by a Polarizable Continuum Dielectric Model. *Chem. Phys. Lett.* **1998**, *286*, 253−260.
(32) Yanai, T.; Tew, D. P.; Handy, N. C. A New Hybrid Exchange−Correlation Functional Using the Coulomb-Attenuating Method (CAM-B3LYP). *Chem. Phys. Lett.* **2004**, *393*, 51−57.
(33) DiLabio, G. A.; Johnson, E. R.; Otero-de-la-Roza, A. Performance of Conventional and Dispersion-Corrected Density-Functional Theory Methods for Hydrogen Bonding Interaction Energies. *Phys. Chem. Chem. Phys.* **2013**, *15*, 12821−12828.
(34) Zhao, Y.; Truhlar, D. G. Density Functionals With Broad Applicability in Chemistry. *Acc. Chem. Res.* **2008**, *41*, 157−167.
(35) Catalán, J.; Palomar, J.; De Paz, J. L. G. Intramolecular Proton or Hydrogen-Atom Transfer in the Ground and Excited States of 2-Hydroxybenzoyl Compounds. *J. Phys. Chem. A* **1997**, *101*, 7914−7921.
(36) Shi, D.; Bradshaw, T. D.; Wrigley, S.; McCall, C. J.; Lelieveld, P.; Fichtner, I.; Stevens, M. F. G. Antitumor Benzothiazoles. 3.[1] Synthesis of 2-(4-Aminophenyl)benzothiazoles and Evaluation of Their Activities against Breast Cancer Cell Lines in Vitro and in Vivo. *J. Med. Chem.* **1996**, *39*, 3375−3384.
(37) Sun, Y.; Zhu, X.; Chen, Z.; Zhang, Y.; Cao, Y. Potential Solution Processible Phosphorescent Iridium Complexes toward Applications in Doped Light-Emitting Diodes: Rapid Syntheses and Optical and Morphological Characterizations. *J. Org. Chem.* **2006**, *71*, 6281−6284.
(38) Wang, H.; Chen, G.; Liu, Y.; Hu, L.; Xu, X.; Ji, S. The Synthesis and Characterization of Novel Dipolar Fluorescent Materials Based on a Quinoxaline Core. *Dyes Pigm.* **2009**, *83*, 269−275.
(39) Wang, Y.; Tan, H.; Liu, Y.; Jiang, C.; Hu, Z.; Zhu, M.; Wang, L.; Zhu, W.; Cao, Y. Synthesis, Opto-Physics, and Electroluminescence of Cyclometalated Iridium (III) Complex with Alkyltrifluorene Picolinic Acid. *Tetrahedron* **2010**, *66*, 1483−1488.
(40) Panthi, K.; El-Khoury, P. Z.; Tarnovsky, A. N.; Kinstle, T. H. Synthesis and Computational Studies of Diphenylamine Donor-Carbazole Linker-Based Donor-Acceptor Compounds. *Tetrahedron* **2010**, *66*, 9641−9649.
(41) Van der Linden, M.; Borsboom, J.; Kaspersen, F.; Kemperman, G. Asymmetric Synthesis of (S)-Mirtazapine: Unexpected Racemization through an Aromatic ipso-Attack Mechanism. *Eur. J. Org. Chem.* **2008**, *2008*, 2989−2997.
(42) Frey, W.; Laermer, F.; Elsaesser, T. Femtosecond Studies of Excited-State Proton and Deuterium Transfer in Benzothiazole Compounds. *J. Phys. Chem.* **1991**, *95*, 10391−10395.

DOI: 10.1021/jp511578v
J. Phys. Chem. C 2015, 119, 4242−4251